Robust spike timing in an excitable cell with delayed feedback

Kyle C. A. Wedgwood[1,*,†], Piotr Słowiński[1,*], James Manson[1], Krasimira Tsaneva–Atanasova[1,3,4], and Bernd Krauskopf[2,5]

[1] *Living Systems Institute and Department of Mathematics, College of Engineering, Mathematics and Physical Sciences, University of Exeter, Stocker Road, Exeter, Devon, EX4 4QD, UK*

[2] *Department of Mathematics, University of Auckland, Auckland, 1010, New Zealand*

[3] *Institute for Advanced Study, Technical University of Munich, Lichtenbergstrasse 2 a, D-85748 Garching, Germany*

[4] *Department of Bioinformatics and Mathematical Modelling, Institute of Biophysics and Biomedical Engineering, Bulgarian Academy of Sciences, 105 Acad. G. Bonchev Str., 1113 Sofia, Bulgaria*

[5] *Dodd-Walls Centre for Photonic and Quantum Technologies, Dunedin 9054, New Zealand*

[*] *Equal contribution*

[†] *Corresponding author*

March 17, 2021

Abstract

The initiation and regeneration of pulsatile activity is a ubiquitous feature observed in excitable systems with delayed feedback. Here, we demonstrate this phenomenon in a real biological cell. We establish a critical role of the delay resulting from the finite propagation speed of electrical impulses on the emergence of persistent multiple-spike patterns. We predict the co-existence of a number of such patterns in a mathematical model and use a biological cell subject to dynamic clamp to confirm our predictions in a living mammalian system. Given the general nature of our mathematical model and experimental system, we believe that our results capture key hallmarks of physiological excitability that are fundamental to information processing.

Keywords: Neuronal excitability, delayed-feedback, mathematical modelling, dynamic clamp

Introduction

Persistent and repetitive electrical spiking activity underlies information processing in a wide range of excitable biological systems, including neurons [1, 2], arthropod muscle fiber [3], cardiac cells [4, 5, 6], pancreatic β-cells and other endocrine cells [7, 8]. Spikes: brief, rapid depolarisations of the voltage across cells membranes, are initiated due to the excitability properties of the cell and in response to incoming stimuli, such as electrical impulses induced by other cells. Excitability properties allow cells to selectively respond to inputs in an 'all-or-none' fashion, acting as a nonlinear filter and enabling precise temporal encoding of stimuli. In certain contexts, spiking patterns induced by transient stimuli are repetitively regenerated following stimulus withdrawal [9], suggesting a mechanism by which memories could be encoded in the timing or frequency of spiking events, as has been postulated for the encoding of sensory inputs and in motor control [10, 11].

Electrical impulses in the brain traverse, via axonal and dendritic projections, distances that can extend many times the cell body. The finite conduction velocity along such projections induces delays in signal transduction and information processing, including in the encoding and decoding of memories [12, 13, 14]. Since delayed spiking activity has been linked to working memory [14], it should come as no surprise that demyelinating diseases, in which the electrical insulation around axons degrades, are associated with memory impairment.

Excitable systems subject to delayed feedback are capable of regenerating their own excitable response, resulting in robust multi-pulse patterns dependent on the feedback strength and the length of the delay interval [15, 16, 17]. The presence of rich dynamics, including co-existence between different types of dynamic behaviour in nonlinear systems with delays [15, 16, 17] has sparked significant interest in investigating the interplay between excitability and delay in a variety of

systems. A prominent example of such a system involves semiconductor micro-cavity lasers [18, 19, 20]; in an analogous fashion to neural systems, the number of emission pulses per delay period in the laser system is thought to be reflective of its ability to store information. In particular, it has been suggested that this property could be used in the construction of bio-inspired 'neuromorphic' photonic resonators that process information through light pulses alone [21, 22]. Supporting this perspective are results that show that pulse-timing patterns due to regeneration of excitation exist in a coherently driven laser [23] and a wavelength tuneable semiconductor laser subject to optoelectronic delayed feedback [24] as well as in a driven laser subject to optoelectronic delayed feedback [25], and a micro-laser with integrated saturable absorber [26]. Given the similarities in excitability between neural and laser systems, it is pertinent to inquire as to which features of the regenerative process are common to both and which differ, noting that such dynamics have previously been observed in delay-coupled recurrent neural loops subject to continuous long-term stimulation [27, 28].

A mathematical description of neuronal excitability by Hodgkin and Huxley [29] paved the way for theoretical investigations of the nonlinear dynamics associated with neural response. Since then, the essence of excitability has been refined into simpler models, such as the FitzHugh–Nagumo model [30, 31] and Morris–Lecar models [3]. Theoretical analysis of such models offers a powerful approach to gain insight into the generation of rhythmic activity in electrically excitable cells by identifying and quantifying the contribution of specific processes to the overall dynamic response. Since the refined models capture the key features of excitability, observations from such analysis can be mapped to a wide range of different cell types.

In this paper, we combine theory and experiments to systematically investigate the interplay between excitability and delayed feedback and its implications for information processing. We append a delayed-feedback term to a well-established, widely-used mathematical model of cellular excitability and use numerical continuation (bifurcation analysis) to characterise the behaviour of the model as the feedback strength and delay period of the feedback are varied. The form of feedback we incorporate has a form akin to that of an *autapse*, which is a chemical synapse from a neuron to itself. Autaptic connections have previously been shown to be important in establishing and maintaining rhythmic activity in mathematical models of small [32] and large [33] neural networks. Here, we investigate the interplay between autaptic processing and excitability dynamics in a single cell. To test our theoretical results, we employ dynamic clamp [34] and confirm our theoretical predictions in a living mammalian system represented by an excitable cell as a natural platform for studying excitation and regeneration patterns.

Theoretical predictions

We adopt the canonical Morris–Lecar (ML) model [3] to describe somatic membrane potential dynamics and extend it with a delayed-feedback term to describe a transient input stimulus to the model cell. The ML model belongs to the general class of Hodgkin–Huxley-type models, which form the basis for almost all biophysical characterisations of electrical excitability in cell membranes [29]. The feedback term incorporates a fixed delay, that could be seen as a representation of conduction delay of the voltage signal, for example. We assume negligible attenuation of the signal and that the delay in the system is due to finite conduction velocity and synaptic transmission. Based on these assumptions, we describe the delayed-feedback via a current-based model of post-synaptic activity with $I_s(t) = \kappa s$ with the dynamics for s given by [35]:

$$\tau_s \dot{s} = s_\infty(V_{\rm pre}) - s, \quad s_\infty(V) = (1+\tanh((V-V_s)/V_h))/2. \tag{1}$$

Here V_s is the threshold for synaptic activation, V_h is the sensitivity of the synapse around the threshold and $V_{\rm pre}$ is the voltage of the pre-synaptic cell, which is the same as the post-synaptic cell in our one cell system. For simplicity, we neglect synaptic dynamics and assume that s is at quasi-steady state but note that the synaptic delay may still be incorporated into τ. These observations allow us to write the current induced by the delayed-feedback as

$$I_s(t) = \kappa\, s_\infty(V(t-\tau)), \tag{2}$$

where the parameter κ scales the feedback strength. This current is added to the standard ionic and applied currents to produce the follow complete model:

$$\begin{aligned} C\dot{V} &= I_{\rm app} - g_{\rm Ca} m_\infty(V)(V - V_{\rm Ca}) - g_{\rm K} w (V - V_{\rm K}) \\ &\qquad - g_{\rm L}(V - V_{\rm L}) + \kappa s(V(t-\tau)), \\ \dot{w} &= \lambda(w)(w_\infty(V) - w), \end{aligned} \tag{3}$$

Table 1: Parameter definitions and values

Parameter	Definition	Value
C	Capacitance of cell membrane (μF/cm^2)	5
ϕ	Time-constant of K^+ channel (ms^{-1})	0.0125
I_{app}	Applied current density (μA/cm^2)	Varies
κ	Gain of delayed synaptic feedback (dimensionless)	Varies
τ	Period of delay (ms)	Varies
g_{Ca}	Conductance of Ca^{2+} channel (mmho/cm^2)	4
g_{K}	Conductance of K^+ channel (mmho/cm^2)	8
g_{L}	Conductance of leak channel (mmho/cm^2)	2
V_{Ca}	Reversal potential of Ca^{2+} channel (mV)	120
V_{K}	Reversal potential of K^+ channel (mV)	-91.89
V_{L}	Reversal potential of leak channel (mV)	-60
V_1	Threshold for Ca^{2+} channel activation (mV)	-2.8
V_2	Sensitivity of Ca^{2+} channel activation (mV)	26
V_3	Threshold for K^+ channel activation (mV)	12
V_4	Sensitivity of K^+ channel activation (mV)	17.4
V_s	Threshold for synaptic activation (mV)	0 (-20 in DC)
V_h	Sensitivity of synaptic activation (mV)	5

where

$$m_\infty(V) = (1 + \tanh((V - V_1)/V_2))/2, \quad (4)$$

$$w_\infty(V) = (1 + \tanh((V - V_3)/V_4))/2, \quad (5)$$

$$\lambda(V) = \phi \cosh((V - V_3)/2V_4), \quad (6)$$

$$s(V) = (1 + \tanh((V - V_s)/V_h)). \quad (7)$$

Parameter definitions and values are listed in Table 1.

Bifurcation analysis

To identify regions of spiking activity in the ML model with delayed-feedback, we appeal to bifurcation theory, which allows for the rapid classification of dynamic behaviour as model parameters are varied. The bifurcation diagram for the system under variation of the feedback strength, κ, and delay, τ, is shown in Fig. 1(a), where we observe coexistence of stable spiking periodic orbits for sufficiently high κ and τ. Along the blue line, we fix $\kappa = 60$ and vary τ, upon which we observe a sequence of bifurcations (folds of periodic orbits) with increasing τ, each of which gives rise to a new pair of spiking solutions, one of which is stable. Fig. 1(b) demonstrates that the branches of stable spiking solutions have approximately equal amplitude (except close to the bifurcation at which they originate), concordant with the intuition that action potentials in an individual cell are stereotyped events so that information is conveyed through spike timing rather than amplitude. In contrast, Fig. 1(c) highlights that the period of the spiking solutions varies significantly between different branches, while depending approximately linearly on the delay τ along each branch. In particular, each stable branch can be mapped to a solution with $n \in \mathbb{N}$ spikes per delay interval, with a common interspike interval (ISI) between each spike.

The number of spikes that can be fitted within the delay interval is limited by the minimal period of spiking activity and the neuron's refractory (or recovery) period (since new action potentials cannot be generated during this time). This imposes limits on the information that can be encoded if one regards spikes as bits of information as suggested in [21, 22]. Examples of stable one-spike (per delay interval) and two-spike (per delay interval) solutions for $\kappa = 60$ and $\tau = 400$ are shown as voltage profiles over two delay intervals in Fig. 1(d) and Fig. 1(e), respectively. The solution to which the system ultimately converges is dependent on the initial condition (given by the history over the delay interval). For a cell initially at rest, this is determined by the timing and form of the current stimulus to which it is exposed. The insets in Fig. 1(d) and Fig. 1(e) depict the Floquet multipliers, which determine the (linear) stability of periodic solutions. We find that the two-spike solution, while indeed stable, possesses a nontrivial multiplier close to the unit circle (the boundary for stability); this scenario is repeated for other n-spike solutions. Hence, equidistant spiking solutions are weakly stable and approached slowly by trajectories over long periods of time.

To examine the effect of multistability on memory encoding, we perform numerical simulations. Here, we use a paired-pulse protocol in which two square-wave current pulses with a finite inter-pulse interval are applied to the cell, as depicted by the purple trace in

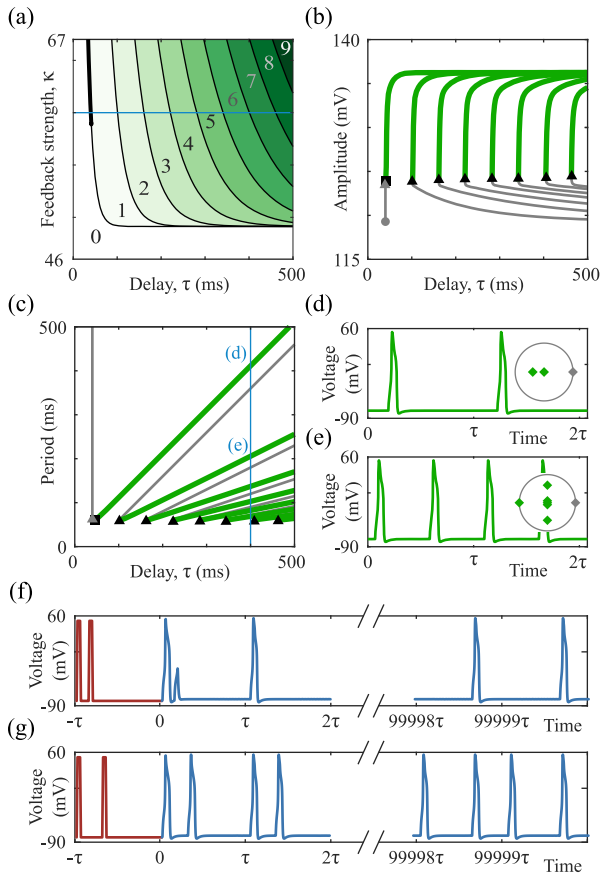

Figure 1: Illustration of co-existence of spiking periodic solutions in the ML model with delayed-feedback. (a)–(c): bifurcation diagrams illustrating how: the number of co-existing periodic solutions (a), their amplitudes (b) and periods (c) depend on the delay, τ (and feedback strength, κ, in (a)). In (a): colours indicate the number (as labelled) of coexisting stable periodic solutions; thin black curves are branches of folds of periodic solutions; the thick black curve is a branch of period-doubling bifurcations; the horizontal blue line indicates $\kappa = 60$ used in (b)–(g). In (b)-(c): symbols indicate bifurcations: dot - homoclinic, triangle - fold of periodic solutions, square - period-doubling; thin grey curves are branches of unstable solutions; thick green curves are branches of stable solutions; the vertical blue line indicates $\tau = 400$ used in (d)–(g). (d)&(e): two out of six co-existing stable periodic solutions for $\kappa = 60$ and $\tau = 400$, with periods of 412 ms (d) and 206 ms (e); time in multiples of τ. The insets illustrate Floquet multipliers: the grey curve is the unit circle, the grey diamond indicates the trivial multiplier 1, and green diamonds depict multipliers of amplitude < 1. (f)&(g): voltage time-traces (blue) of simulations initiated with different initial stimuli (red); pulse width 16 ms; initial inter-spike interval of 56 ms (f) and 120 ms (g).

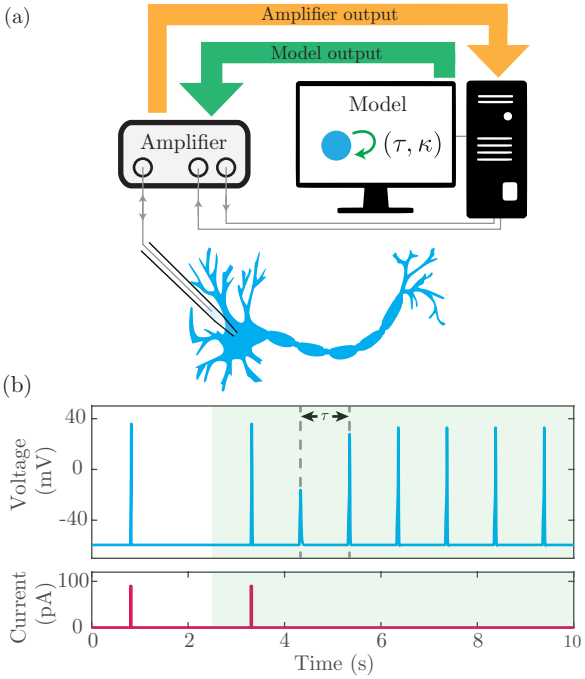

Figure 2: Schematic representation of the dynamic clamp experimental system. (a): A whole-cell patch clamp protocol is used to obtain intracellular access to the cell. In current clamp mode, the voltage of the cell as recorded by the amplifier is used as the input to a mathematical model. This model computes a current that describes the delayed-synaptic feedback term, parametrised by the delay, τ, and the gain, κ, which is subsequently sent back to the amplifier and injected into the cell. (b): In silico simulations of the ML model demonstrate the establishment of self-sustained spiking activity when the feedback is active. The top trace shows the voltage of the cell whilst the bottom trace is an externally provided current input to induce initial excitation in the cell. In the unshaded region, the feedback is inactive ($\kappa = 0$). Here, a current pulse induces a single spike, after which the cell returns to rest. In the shaded region, the feedback is active ($\kappa = 60$) and repetitive spiking activity with a period approximately equal to the delay interval is observed even though only one input current pulse is issued. The delay, τ, is marked in the upper trace for reference.

Fig. 1(f) and Fig. 1(g). Following these initial pulses, no other external inputs are applied to the system. In Fig. 1(f), the first current pulse elicits a full amplitude spike, but the second does not, because it falls into the refractory period of the action potential. During the second delay interval after the initial excitation, the response of the system to the second current pulse has decayed entirely and the trajectory settles rapidly into a one-spike solution. In Fig. 1(g), the interval between the two current input pulses is well beyond the refractory period, and they both elicit large-amplitude action potentials that persist in subsequent delay intervals with heterogeneous ISI patterns (i.e., non-equispaced in time) approximately conserved across many subsequent delay intervals. Nevertheless, the effect of the weak convergence to the stable solution (Fig. 1(e)) is evident: ultimately, the neuron settles to the stable solution with two equally spaced spikes in a similar manner to that observed in laser systems [20].

Experimental verification

We next seek to test our theoretical predictions in an excitable mammalian cell (a GH4 cell; see Materials and Methods) by using the dynamic clamp technique to control the delay time and feedback strength. Dynamic clamp is an electrophysiological technique used to manipulate the excitability properties of individual cells [36, 34]. It is typically used to modify the activity of ion channels (the primary drivers of spiking behaviour) according to pre-defined mathematical models, which allows one to quantify their contribution to overall excitability [37]. Here, we use it to apply delayed-feedback to an isolated cell. In this way, the spike generating mechanisms of the cell are preserved, whilst parameters of the feedback are directly modifiable during the experiment. A schematic of the dynamic clamp protocol is shown in Fig. 2(a). Briefly, the voltage signal recorded via the amplifier is used as an input to our mathematical model of the delayed-feedback, (2). The resulting feedback current is sent back to the amplifier to be injected into the cell to provide real-time closed-loop feedback.

Synthetic data from the augmented ML model are shown in Figure 2(b), in which we apply a solitary current pulse to the cell of sufficient amplitude and duration to trigger a spike. In the unshaded region, the feedback term is absent (i.e., the synaptic gain is $\kappa = 0$). Following the first spike, which occurs in direct response to the current pulse, the cell returns to rest. In the shaded region, the gain is now set to $\kappa = 60$. Now, after the application of the initial current pulse and subsequent spike, recurrent excitation builds up in the cell and self-sustained spiking activity is generated with a period approximately equal to the delay interval.

We experimentally emulate the paired-pulse protocol performed in the mathematical model in Fig. 1(f), Fig. 1(g) and Fig. 2(b) in a real cell. The results of a typical experiment are shown in Fig. 3, with full traces displayed in Figs. S1-S3 in the Supplementary Materials. The left-hand column of Fig. 3 shows the first 8 seconds of the overall recording, including the initial current pulse. To facilitate viewing, the green and orange arrows above the spikes indicate by which initial current pulse they were originally generated; the right-hand column of Fig. 3 shows the same data in a pseudo-space plot where the respective time series is folded over the delay interval to show the evolution of pulses in the delay interval from cycle-to-cycle. In Fig. 3(a)-(b), the synaptic gain is set to $\kappa = 40$, which is not large enough for the initial current pulses to generate self-sustained activity, and the cell returns to rest. Upon setting $\kappa = 60$, the spikes produced by the initial current pulse (indicated with an orange arrow) die out, whilst those produced by the second current pulse (indicated with a green arrow) grow in amplitude until self-sustained spiking activity with one spike per delay interval is obtained, as shown in Fig. 3(c)-(d), echoing the findings in Fig. 1(f). Keeping $\kappa = 60$ but increasing the inter-pulse interval results, as reported in Fig. 3(e)-(f), in the growth of action potentials generated by both initial current pulses until recurrent activity with two spikes per delay interval is established, thus, recapitulating the result from Fig. 1(g). This experiment highlights the capability of the cell to encode distinct and persistent multi-spike rhythms (activity patterns) and confirms the predictions from the analysis of the mathematical model.

Discussion

In this study, we demonstrate that a single excitable cell with delayed self-feedback is a rhythm-generating system capable of sustaining regular spiking oscillations of different periods in response to an initial excitation pattern. The number of distinct patterns that can be realised by the neuron is heavily dependent on the strength and delay interval of the self-feedback. In

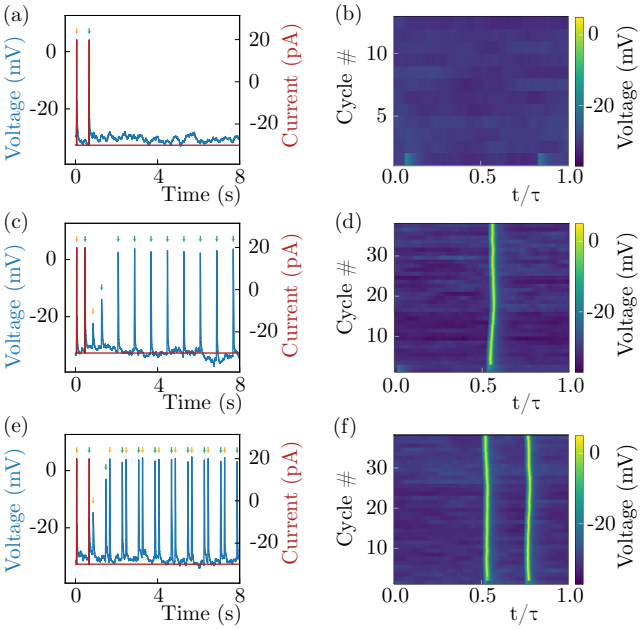

Figure 3: Summary of paired-pulse experiments. Panels (a), (c) &(e) represent the voltage dynamics (blue) of a cell in response to a paired current pulse (red). In each experiment, an initial current pulse is followed after some time by a second current pulse. In panels (a)-(b), $\kappa = 40$, whilst $\kappa = 60$ in all other panels. Across the entire experiment, the delay is fixed at $\tau = 800$. The inter-pulse interval was set to 600 ms in panels (a) & (e) and 400 ms in panel (c) (and the same for the corresponding plots to their right). The orange and green arrows above the spikes indicate which initial current pulse induced the spiking behaviour. Observe that in panel (c), the spikes induced by the orange pulse, alone, die out, whilst the ones induced by the green pulse grow and ultimately give rise to a self-sustained oscillation with one spike per delay interval. This is in contrast to panel (e) in which the spikes induced by both the orange and green pulse are sustained, resulting in a two-spike per delay interval pattern. Panels (b), (d) & (f) show the same data as the panels above them but with the time series plotted against successive cycles of the delay interval.

particular, if the feedback strength is too low, the excitation in the cell cannot be regenerated and no persistent activity is generated. If the feedback strength is sufficiently high, the number of supported patterns increases with the delay interval. This latter observation results from the interplay between excitability properties and the delay: the number of spikes that can be accommodated over a fixed delay is limited by the cell's spiking and refractory periods. Mathematical analysis of such dynamic behaviours makes these observations rigorous, whereupon we find that the generation of each spiking pattern can be attributed to a specific bifurcation. Which of the potentially many spiking patterns is ultimately observed depends on the initial stimulus. The mathematical model predicts that changing the inter-pulse interval in a paired-pulse stimulus experiment is sufficient to switch the resulting activity pattern from a one-spike per delay interval to a two-spike per delay interval solution. The corroboration of these results in a real cell confirms these predictions and validates the modelling approach.

In the experimental verification of our model predictions, we showed that the delayed feedback of the form chosen is sufficient to produce stable rythms with one-spike and two-spike per delay period. Our bifurcation analysis demonstrated that the associated periodic solutions possess Floquet multipliers close to (but inside) the unit circle, suggesting slow rates of attraction to equidistant pulsing rythms. Additionally, biological systems display considerable complexity and heterogeneity. In particular, neurons are well-known to exhibit different classes of excitability [38], and may generate complex spiking rhythms even in the absence of external input or feedback [39, 40]. It is therefore a pertinent question for careful future attention to inquire how robust such multiple-spike solutions are in real cells. In this direction, we make two remarks. Firstly, our model of choice is general in that we did not tune our analysis to any particular cell type. Moreover, the Morris–Lecar model can, in different parameter regimes, exhibit properties of the different excitability classes. As such, our framework provides flexibility to explore such avenues. Secondly, whilst repetitive activity of the kind we discuss here may be fragile in certain experimental systems, recent work in laser physics found sufficiently large parameter ranges over which different multiple pulse rhythms due to excitability and delayed feedback can be found stably over very large timescales [20, 41]. This suggests that these dynamics may be quite robust in practice also when the excitable element is a cell of suitable

type. A more detailed investigation of how multiple-spike rythms of the clamped cell experiment depend on the properties of the feedback loop, as well as those of the cell itself, is a challenging task and the subject of ongoing research.

Given the nature of the Hodgkin–Huxley-type model and of the experimental setup, we believe that our results capture key hallmarks of physiological excitability fundamental to neural processing in a wide array of contexts. Notably, the striking similarity between the theoretical predictions and experimental data were not produced by fitting a specific mathematical model to the chosen cell type, but were reflective of general properties of excitability that are present in most neurons, as well as other cell types [4, 5, 6, 7, 8]. The parallels of our results with those observed in laser systems [18, 20] further highlight the ubiquitous nature of the regeneration of activity in excitable systems with delay. Our experimental setup showcases that a living mammalian system, represented by an excitable cell, is a feasible platform for studying this phenomenon in a neural context. The framework we have established is flexible and will allow further exploration of the interplay between delay and important biophysical aspects such as the aforementioned role of different excitability sub-classes, and of complex intrinsic spiking patterns.

The ability to control multi-spike behaviour in biological cells more widely opens a new avenue towards investigating how memories can be robustly encoded. This may well have significant implications for better understanding not only normal brain function [42], but also debilitating conditions such as Alzheimer's Disease [43, 44]. Knowledge of the interplay between excitability and delay is also crucial for designing effective stimulation protocols for brain–machine interfaces. We expect that these issues, among others, will dictate how delays can be incorporated in useful devices based on excitable systems, whether in the neurological, sensory, motor, or other domains.

Materials and methods

Bifurcation analysis Bifurcation analysis was performed with the package DDE-BIFTOOL v3.1.1 (http://ddebiftool.sourceforge.net) in Matlab R2020a (https://uk.mathworks.com) on a standard laptop computer. Branches of codimension-one bifurcations of periodic orbits (folds of periodic orbits, period-doubling bifurcations) were computed with the extension debiftool_extra_psol [45, 46]. Code to produce the bifurcation diagrams and replicate model simulations may be downloaded from the GitHub repository (https://github.com/SlowinskiPiotr/MorrisLecarDDE).

Cell culture The rat norvegicus pituitary tumor GH4C1 (GH4) cell line was cultured in Hams F-10 nutrient mixture (81.5%), supplemented with horse serum (15%), FBS (2.5%) and Glutamax (1%). Cells were thawed following standard procedures and cultured for 2 weeks in a 5% CO2 incubator at 37°C, passaging every 3-4 days in T75 vented flasks. Prior to experimentation, cells were transferred to 15 mm glass cover slips for patching, seeded at a sufficiently low density to easily identify isolated cells. Immediately prior to experimentation, cells were washed three times in PBS to remove any residual serum.

Patching solutions The extracellular solution was comprised of 2.8 mM glucose, 132 mM NaCl, 5 mM KCl, 2.6 mM $CaCl_2$, 1.2 mM $MgCl_2$, 10 mM HEPES, 100 μM paxilline (pH 7.4 adjusted with NaOH, osmolarity 295 mOsm/L adjusted with sucrose). Paxilline was added to the solution to block BK channels to reduce the probability of bursting activity typically seen in GH4 cells [47].

The intracellular solution was comprised of 100 mM K-gluconate, 20 mM KCl, 4 mM NaCl, 1 mM $CaCl_2$, 4 mM $MgCl_2$, 10 mM EGTA, 10 mM HEPES (pH 7.2 adjusted with KOH, osmolarity 285 mOsm/L adjusted with sucrose). Immediately before patching, amphotericin B (Sigma) was added to the internal solution at a final concentration of 0.6 mg/mL. When not in use, the internal solution was kept on ice and away from light.

Patching equipment Recordings were taken with a MutliClamp 700A amplifier (Molecular Devices, https://www.moleculardevices.com) and a NIDAQ 6363 (National Instruments, https://www.ni.com/en-gb.html). Stimulation and recording protocols were performed with the Matlab-based Symphony software (OpenEphys, https://open-ephys.org/symphony). Data were analysed with bespoke python code (Anaconda, python 3.6.3, https://anaconda.org).

Dynamic clamp Dynamic clamp was achieved through the Teensy 3.6-based breadboard circuit as presented in [34] with updates as presented at the homepage for that project

(www.dynamicclamp.com/updates). Computer code to simulate the delayed synapse model was developed in Arduino and can be downloaded from the GitHub repository (https://github.com/SlowinskiPiotr/MorrisLecarDDE). To account for the more depolarised membrane potential of the GH4 cells relative to the Morris–Lecar model, the value of V_s in the experiments was set to -20 mV. The Teensy device was controlled by bespoke software developed in Matlab which is freely available at www.github.com/Kyle-Wedgwood/DynamicClampController.

Protocol On the day of recording, thick walled patch pipettes were pulled to a resistance of ~ 3.0 MΩ and subsequently fire polished. Cover slips were loaded into the recording chamber and allowed to settle for 5 min under constant perfusion at 1.5 mL/min in external solution. During this period, isolated cells were marked as candidates for patching. Following the settling period, pipettes were front-filled for 10 s with internal solution without amphotericin B and subsequently back-filled with amphotericin B containing internal solution. Perforated whole-cell patch clamp was then achieved within 60s of filling the pipette, with seals of > 5 GΩ achieved. Perforation was continued until the series resistance fell below 20 MΩ, which took around 15 min.

Following successful perforated patch, the amplifier was switched to current clamp. Bridge balance was applied to compensate for residual series resistance. Initial gap free recordings were obtained to verify that cells were capable of spiking activity. Following this, a holding current of -30 pA was applied to silence spontaneous spiking activity. Paired pulses of 10 ms duration and 50 pA amplitude with varying interpulse intervals ranging from 200 - 600 ms were applied to the cell. Following the initial pulses, recordings were continued for a further 30s. Recordings were taken at a temperature of 34-36°C with a sampling frequency of 20 kHz and filtered with a Bessel filter at 2.8 kHz. Throughout the recordings, the delay period was set to 800 ms and the feedback gain was set to either 40 or 60.

Acknowledgments

We thank Joël Tabak for gifting the GH4 cells used in this study, Andrew Randall for help in setting up the electrophysiology rig, Niraj Desai for help with calibrating the dynamic clamp system and two anonymous referees for their suggestions for manuscript improvements. **Funding statement:** K.C.A.W. graciously acknowledges funding from the MRC Fellowship MR/P01478X/1. The work of P.S. was generously supported by the Wellcome Trust Institutional Strategic Support Award 204909/Z/16/Z. K.T-A. gratefully acknowledges the financial support of the EPSRC via grant EP/N014391/1 and the support of the Technical University of Munich – Institute for Advanced Study, funded by the German Excellence Initiative. B.K. gratefully acknowledges financial support from Royal Society Te Apārangi Marsden Fund grant #19-UOA-223. **Data and materials availability:** Data and computer code related to the mathematical model and dynamic clamp experiments can be downloaded from the GitHub repository https://github.com/SlowinskiPiotr/MorrisLecarDDE. **Author contributions**: K.C.A.W and P.S contribued equally to this work. K.C.A.W carried out the electrophysiology experiments and performed initial mathematical modelling, P.S. and J.M. performed the bifurcation analysis, and K.T-A. and B.K. devised the study. All authors contributed to the writing and revision of the manuscript.

References

[1] R. Chaudhuri and I. Fiete, "Computational principles of memory," *Nature Neuroscience*, vol. 19, no. 3, p. 394, 2016.

[2] E. M. Izhikevich, *Dynamical Systems in Neuroscience*. MIT press, 2007.

[3] C. Morris and H. Lecar, "Voltage oscillations in the barnacle giant muscle fiber," *Biophysical Journal*, vol. 35, no. 1, pp. 193–213, 1981.

[4] D. Noble, "A modification of the hodgkin—huxley equations applicable to purkinje fibre action and pacemaker potentials," *The Journal of Physiology*, vol. 160, no. 2, p. 317, 1962.

[5] D. Barkley, "A model for fast computer simulation of waves in excitable media," *Physica D: Nonlinear Phenomena*, vol. 49, no. 1-2, pp. 61–70, 1991.

[6] A. Karma, "Spiral breakup in model equations of action potential propagation in cardiac tissue," *Physical Review Letters*, vol. 71, no. 7, p. 1103, 1993.

[7] T. R. Chay and J. Keizer, "Minimal model for membrane oscillations in the pancreatic beta-cell," *Biophysical Journal*, vol. 42, no. 2, pp. 181–189, 1983.

[8] H. M. Osinga, A. Sherman, and K. Tsaneva-Atanasova, "Cross-currents between biology and mathematics: The codimension of pseudo-plateau bursting," *Discrete and Continuous Dynamical Systems. Series A*, vol. 32, no. 8, p. 2853, 2012.

[9] A. V. Egorov, B. N. Hamam, E. Fransén, M. E. Hasselmo, and A. A. Alonso, "Graded persistent activity in entorhinal cortex neurons," *Nature*, vol. 420, no. 6912, pp. 173–178, 2002.

[10] S. M. Bothe, "The evidence for neural information processing with precise spike-times: A survey," *Natural Computing*, vol. 3, pp. 195–206, 2004.

[11] C. Kayser, N. K. Logothetis, and S. Panzeri, "Millisecond encoding precision of auditory cortex neurons," *Proceedings of the National Academy of Sciences of the United States of America*, vol. 107, no. 39, pp. 16976–16981, 2010.

[12] S. G. Waxman, "Integrative properties and design principles of axons," in *International Review of Neurobiology*, vol. 18, pp. 1–40, Elsevier, 1975.

[13] H. A. Swadlow, "Impulse conduction in the mammalian brain: physiological properties of individual axons monitored for several months," *Science*, vol. 218, no. 4575, pp. 911–913, 1982.

[14] K. K. Sreenivasan and M. D'Esposito, "The what, where and how of delay activity," *Nature Reviews Neuroscience*, vol. 20, no. 8, pp. 466–481, 2019.

[15] K. Ikeda, K. Kondo, and O. Akimoto, "Successive higher-harmonic bifurcations in systems with delayed feedback," *Physical Review Letters*, vol. 49, no. 20, p. 1467, 1982.

[16] S. Yanchuk and P. Perlikowski, "Delay and periodicity," *Physical Review E*, vol. 79, no. 4, p. 046221, 2009.

[17] S. Yanchuk, S. Ruschel, J. Sieber, and M. Wolfrum, "Temporal dissipative solitons in time-delay feedback systems," *Physical Review Letters*, vol. 123, no. 5, p. 053901, 2019.

[18] S. Terrien, B. Krauskopf, N. G. R. Broderick, R. Braive, G. Beaudoin, I. Sagnes, and S. Barbay, "Pulse train interaction and control in a microcavity laser with delayed optical feedback," *Optics Letters*, vol. 43, no. 13, pp. 3013–3016, 2018.

[19] K. Lüdge, L. Jaurigue, B. Lingnau, S. Terrien, and B. Krauskopf, "Semiconductor mode-locked laser with external feedback: emergence of multi-frequency pulse trains with an increasing number of modes," *The European Physical Journal B*, vol. 92, no. 4, p. 89, 2019.

[20] S. Terrien, V. A. Pammi, N. G. R. Broderick, R. Braive, G. Beaudoin, I. Sagnes, B. Krauskopf, and S. Barbay, "Equalization of pulse timings in an excitable microlaser system with delay," *Physical Review Research*, vol. 2, p. 023012, 2020.

[21] B. Romeira, R. Avó, J. M. Figueiredo, S. Barland, and J. Javaloyes, "Regenerative memory in time-delayed neuromorphic photonic resonators," *Scientific Reports*, vol. 6, p. 19510, 2016.

[22] B. Romeira, J. M. Figueiredo, and J. Javaloyes, "Delay dynamics of neuromorphic optoelectronic nanoscale resonators: Perspectives and applications," *Chaos: An Interdisciplinary Journal of Nonlinear Science*, vol. 27, no. 11, p. 114323, 2017.

[23] B. Garbin, J. Javaloyes, G. Tissoni, and S. Barland, "Topological solitons as addressable phase bits in a driven laser," *Nature Communications*, vol. 6, no. 1, pp. 1–7, 2015.

[24] L. Larger, B. Penkovsky, and Y. Maistrenko, "Laser chimeras as a paradigm for multistable patterns in complex systems," *Nature Communications*, vol. 6, no. 1, pp. 1–7, 2015.

[25] F. Marino and G. Giacomelli, "Pseudo-spatial coherence resonance in an excitable laser with long delayed feedback," *Chaos: An Interdisciplinary Journal of Nonlinear Science*, vol. 27, no. 11, p. 114302, 2017.

[26] S. Terrien, B. Krauskopf, N. G. R. Broderick, L. Andréoli, F. Selmi, R. Braive, G. Beaudoin, I. Sagnes, and S. Barbay, "Asymmetric noise sensitivity of pulse trains in an excitable microlaser with delayed optical feedback," *Physical Review A*, vol. 96, no. 4, p. 043863, 2017.

[27] J. Foss, A. Longtin, B. Mensour, and J. Milton, "Multistability and delayed recurrent loops," *Physical Review Letters*, vol. 76, no. 4, p. 708, 1996.

[28] J. Foss and J. Milton, "Multistability in recurrent neural loops arising from delay," *Journal of Neurophysiology*, vol. 84, no. 2, pp. 975–985, 2000.

[29] A. L. Hodgkin and A. F. Huxley, "A quantitative description of membrane current and its application to conduction and excitation in nerve," *The Journal of Physiology*, vol. 117, no. 4, p. 500, 1952.

[30] R. FitzHugh, "Mathematical models of threshold phenomena in the nerve membrane," *The Bulletin of Mathematical Biophysics*, vol. 17, no. 4, pp. 257–278, 1955.

[31] R. FitzHugh, "Impulses and physiological states in theoretical models of nerve membrane," *Biophysical Journal*, vol. 1, no. 6, p. 445, 1961.

[32] Y. Zhou, T. Vo, H. G. Rotstein, M. M. McCarthy, and N. Kopell, "M-Current Expands the Range of Gamma Frequency Inputs to Which a Neuronal Target Entrains," *Journal of Mathematical Neuroscience*, vol. 8, no. 1, pp. 1–32, 2018.

[33] P. R. Protachevicz, K. C. Iarosz, I. L. Caldas, C. G. Antonopoulos, A. M. Batista, and J. Kurths, "Influence of Autapses on Synchronization in Neural Networks With Chemical Synapses," *Frontiers in Systems Neuroscience*, vol. 14, no. November, pp. 1–13, 2020.

[34] N. S. Desai, R. Gray, and D. Johnston, "A dynamic clamp on every rig," *eNeuro*, vol. 4, no. 5, 2017.

[35] C. Börgers, S. Epstein, and N. J. Kopell, "Background gamma rhythmicity and attention in cortical local circuits: a computational study," *Proceedings of the National Academy of Sciences*, vol. 102, no. 19, pp. 7002–7007, 2005.

[36] A. A. Prinz, L. F. Abbott, and E. Marder, "The dynamic clamp comes of age," *Trends in Neurosciences*, vol. 27, no. 4, pp. 218–224, 2004.

[37] H. Ori, H. Hazan, E. Marder, and S. Marom, "Dynamic clamp constructed phase diagram for the Hodgkin and Huxley model of excitability," *Proceedings of the National Academy of Sciences of the United States of America*, vol. 117, no. 7, pp. 3575–3582, 2020.

[38] S. A. Prescott, "Excitability: Types i, ii, and iii," in *Encyclopedia of Computational Neuroscience* (D. Jaeger and R. Jung, eds.), pp. 1–7, New York, NY: Springer New York, 2013.

[39] E. M. Izhikevich, "Neural excitability, spiking and bursting," *International Journal of Bifurcation and Chaos*, vol. 10, no. 6, pp. 1171–1266, 2000.

[40] F. Zeldenrust, W. J. Wadman, and B. Englitz, "Neural coding with bursts—current state and future perspectives," *Frontiers in Computational Neuroscience*, vol. 12, p. 48, 2018.

[41] S. Terrien, V. A. Pammi, B. Krauskopf, N. G. R. Broderick, and S. Barbay, "Pulse-timing symmetry breaking in an excitable optical system with delay," *Physical Review E*, vol. 103, p. 012210, 2021.

[42] J. Jonides, R. L. Lewis, D. E. Nee, C. A. Lustig, M. G. Berman, and K. S. Moore, "The mind and brain of short-term memory," *Annual Review of Psychology*, vol. 59, pp. 193–224, 2008.

[43] C. L. Grady, M. L. Furey, P. Pietrini, B. Horwitz, and S. I. Rapoport, "Altered brain functional connectivity and impaired short-term memory in alzheimer's disease," *Brain*, vol. 124, no. 4, pp. 739–756, 2001.

[44] M. A. Parra, S. Abrahams, K. Fabi, R. Logie, S. Luzzi, and S. D. Sala, "Short-term memory binding deficits in alzheimer's disease," *Brain*, vol. 132, no. 4, pp. 1057–1066, 2009.

[45] J. Sieber, "Extended Systems for bifurcations of periodic orbits in delay differential equations," 7 2013. https://figshare.com/articles/journal_contribution/Extended_Systems_for_bifurcations_of_periodic_orbits_in_delay_differential_equations/757725.

[46] K. Engelborghs, T. Luzyanina, and D. Roose, "Numerical bifurcation analysis of delay differential equations using dde-biftool," *ACM Transactions on Mathematical Software (TOMS)*, vol. 28, no. 1, pp. 1–21, 2002.

[47] J. Tabak, M. Tomaiuolo, A. E. Gonzalez-Iglesias, L. S. Milescu, and R. Bertram, "Fast-activating voltage-and calcium-dependent potassium (BK) conductance promotes bursting in pituitary cells: A dynamic clamp study," *Journal of Neuroscience*, vol. 31, no. 46, pp. 16855–16863, 2011.